Desalination and Water Treatment
www.deswater.com
doi: 10.1080/19443994.2014.985727

57 (2016) 3317–3327
February

Taylor & Francis
Taylor & Francis Group

Gypsum scaling during forward osmosis process—a direct microscopic observation study

Minmin Zhang[a,b], Junhong Shan[a,b], Chuyang Y. Tang[c,*]

[a]*School of Civil & Environmental Engineering, Nanyang Technological University, Singapore 639798, Singapore, Tel. +65 84301086; email: mzhang6@e.ntu.edu.sg (M. Zhang), Tel. +65 66011664; email: erisj@nus.edu.sg (J. Shan)*
[b]*Singapore Membrane Technology Centre, Nanyang Technological University, Singapore 639798, Singapore*
[c]*Department of Civil Engineering, University of Hong Kong, HW-619B Haking Wong Building, Pokfulam, Hong Kong, Tel. +852 8591976; Fax: +852 25595337; email: tangc@hku.hk*

Received 11 April 2014; Accepted 31 October 2014

ABSTRACT

This study investigated the effect of supersaturation index (SI), ionic strength, membrane orientation, and antiscalant (AS) addition on gypsum scaling during forward osmosis (FO) desalination. Scaling tests were performed in a cross-flow FO system, and the development of gypsum scalants on FO membrane was directly observed using an optical microscope integrated with the FO filtration cell. Greater surface coverage by gypsum crystals and larger crystal sizes occurred on the scaled FO membranes for feed solutions (FS) with higher SI values accompanying with more severe flux reduction. At fixed Ca^{2+} and SO_4^{2-} concentrations, reducing the ionic strength of the FS from 0.55 to 0.15 M resulted in longer induction time. Nevertheless, more flux loss and surface coverage by scalants occurred at longer filtration duration for 0.15 M FS due to its greater ion activities and thus higher SI. The active layer facing (AL)-draw solution membrane orientation was found to be prone to internal scaling, which is likely as a result of unfavorable internal concentration polarization of scaling precursors inside the FO membrane support layer. On contrary, the AL-FS orientation had much more stable flux behavior. The current study also demonstrated the effectiveness of AS addition and rinsing under cross-flow conditions for FO scaling control.

Keywords: Forward osmosis (FO); Desalination; Gypsum scaling; Supersaturation index; Antiscalant; Direct microscopic observation

1. Introduction

Forward osmosis (FO) is a process where a semi-permeable dense membrane separates a low concentration FS and a high concentration draw solution (DS) [1–3]. During the operation of FO, water flows though the membrane from the FS to the DS under the osmotic pressure driving force [4,5]. In recent years, FO process experienced rapid developments due to its potentially low energy consumption, as well as its lower fouling propensity [6,7], compared with pressure driven membrane process [1]. Potential applications of FO include water and wastewater treatment [8–10], desalination [11–13], and power generation using related pressure retarded osmosis (PRO) process [14–16].

*Corresponding author.

Reverse osmosis (RO) process technology has been well developed to solve drinking water shortage problems based on seawater desalination. In RO, fouling (particularly scaling) is the most commonly encountered problem that limits water recovery [17,18]. Many works have focused on the mechanisms of RO scaling (e.g. gypsum ($CaSO_4{\cdot}2H_2O$) scaling) and methods to alleviate scaling [19–22]. In comparison to the more established RO desalination, FO desalination is an emergent topic [23,24]. The performance of FO process can be similarly limited by membrane fouling [25–28]. In particular, the application of FO for seawater desalination can be potentially limited by gypsum scaling [27,29]. So far, only a few studies have investigated FO scaling and scaling inhibition. Mi and Elimelech [27] investigated the mechanisms of gypsum scaling and cleaning in both FO and RO by comparing their water flux behavior and atomic force microscopic adhesion force measurements. They further investigated the role of membrane chemistry and demonstrated that polyamide membrane experienced severe scaling than cellulose acetate membrane when operating in FO mode. Working temperature can also affect membrane scaling in FO process as it relates to mass transfer, mineral solubility limit, and concentration polarization [28,30]. Besides, the presence of other types of organic foulant will also affect scaling phenomena where accelerated gypsum crystallization process was found to promote gypsum crystal growth [31,32], in the study of combined organic-inorganic fouling of FO membranes. Whereas many prior scaling studies investigated membrane flux behavior, non-invasive direct microscopic observation can provide complementary information on fouling formation and development in both RO [33] and FO [31,34] processes. In addition, the effectiveness of antiscalants (ASs) in FO scaling control is seldom reported [19]. Direct microscopic observation can be a convenient way to assess the effectiveness of AS dosing.

The objective of the current study was to investigate the factors affecting gypsum scaling in FO process based on FO flux measurements as well as direct microscopic observation. Parameters studied include supersaturation index (SI) of gypsum, ionic strength (IS) of FS, and membrane orientation. The effectiveness of the addition of AS and rinsing under cross-flow conditions were also tested. The current study may provide important insight for FO scaling and scaling control.

2. Materials and methods

2.1. Chemicals and solution chemistry

Synthetic seawater (Table 1) was prepared from reagent-grade calcium chloride ($CaCl_2{\cdot}2H_2O$), magnesium chloride ($MgCl_2{\cdot}6H_2O$), sodium chloride (NaCl), and anhydrous sodium sulfate (Na_2SO_4) in accordance to ASTM Method D1141-98 [35] and was used as a reference FS. The effect of SI was investigated by varying the concentrations of calcium chloride and sodium sulfate while keeping the ionic strength at the reference level of 0.55 M by adjusting the sodium chloride concentration accordingly. In the current study, SI is defined according to Eq. (1) [36]:

Table 1
Composition of model solution used in the experiment for FO scaling

Ions	Model solution
Na^+	11,025.9 mg/L
Mg^{2+}	1,313.7 mg/L
Ca^{2+}	418 mg/L
Cl^-	32,702.7 mg/L
SO_4^{2-}	2,765.1 mg/L
Osmotic pressure	25.5 atm
SI_{gypsum}	0.21
pH	7.5
Ionic strength	0.55 M

$$SI_g = \frac{(Ca^{2+})(SO_4^{2-})}{K_{sp}} \quad (1)$$

where (Ca^{2+}) and (SO_4^{2-}) are the activities of the calcium and sulfate ions, respectively, and K_{sp} is the thermodynamic solubility constant for gypsum. The saturation index values were calculated using the OLI stream analyzer software (OLI Systems, Inc., Morris Plains, NJ) [37].

The effect of AS was evaluated using commercially available Flocon 260 (Water Additives Inc.). According to the manufacturer, Flocon 260 contains a mixture of polycarboxylic acids. These polycarboxylic acids are good chelating agents for multivalent cations [38,39].

2.2. FO membranes

A commercial cellulose triacetate (CTA) FO membrane, named as CTA-W according to our previous study [40], were used in the current study. The membrane was provided by Hydration Technologies, Inc. (Albany, OR). The membrane has an asymmetric structure and is supported by embedded polyester meshes [40,41]. According to our prior study [40], it has an overall thickness of ~45 μm and porosity of 46% [40]. Its water permeability and NaCl permeability coefficient were 9×10^{-13} m/s Pa and 4×10^{-13} m/s, respectively.

2.3. FO experiments

FO scaling tests were performed with a bench-scale FO membrane system (Fig. 1). For each test, a new membrane coupon (effective area = 36.1 cm^2) was housed in a cross-flow membrane cell. Diamond-patterned spacers were placed on both sides of the membrane to enhance the support of the membrane as well as to improve flow distribution. A multiple-channel variable-speed pump (Masterflex, Cole Parmer, USA) was used to control the cross-flow velocity of both FS and DS. A dampener was placed after the pump to minimize flow pulsation.

The membrane was first equilibrated with background electrolyte solution under cross-flow conditions for 20 min. Calcium chloride was then added into the FS to start the scaling experiment. FO flux was determined by measuring the weight changes of the FS at regular time intervals using a digital balance (Mettler-Toledo). Unless specified otherwise, the active layer facing FS (AL-FS) orientation was used. The draw solution containing 4 M NaCl was used for AL-FS orientation experiments. The cross-flow velocity was maintained at 9.75 cm/s for both FS and DS. FS pH and temperature were kept at 7.5 and 23 ± 1°C, respectively. The scaling test was performed for 6 h or when flux decline reached >60%. AS (Flocon 260) was added in some scaling tests to assess its effectiveness for controlling FO scaling. In addition, rinsing with deionized water was also conducted under cross-flow conditions to evaluate its cleaning efficiency. During this cleaning stage, the cross-flow velocity was increased to 19.5 cm/s to enhance the cleaning efficiency.

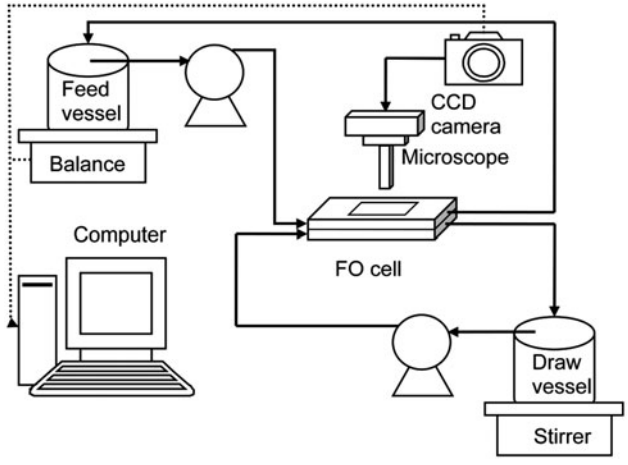

Fig. 1. Schematic of the FO cross-flow setup equipped with a direct optical microscopic observation system.

Details of the direct microscopic observation system have been reported by Wang et al. [34]. Briefly, gypsum scaling was observed using a microscope objective lens (10× magnification, Axiolab, Carl Zeiss) placed on the feed side. Optical microscopic images were captured using a high-resolution color CCD camera (JVC, model TK-C921BEG). These images were converted to binary black and white images based on the previously reported procedures [34,41] to allow the determination of membrane surface coverage by the gypsum scalant. The contribution of membrane support mesh was eliminated by subtracting the image of original clean membrane. Scaled membranes were also examined using a Zeiss EVO 50 Scanning Electron Microscope (Carl Zeiss Pte. Ltd). In addition, the crystalline phase of the scalant was examined using X-ray powder diffraction (Shimadzu SRD-6000 X-ray diffractometer).

3. Results and discussion

3.1. Direct microscope observation of FO membrane scaling

The direct microscopic observation method was used to monitor gypsum scaling over time. The captured optical micrographs of the fouled CTA-W membrane clearly showed the appearance and development of scaling on the membrane surface (Fig. 2). For a FS SI of 1.97, negligible amount of the gypsum crystals were observed in the first two hours of the scaling test. Significant scaling occurred only at longer duration (see micrographs at 4 and 6 h in Fig. 2(a). These crystals were confirmed to be gypsum based on XRD analysis (Fig. A in the appendix). When an SI of 2.44 was used, scaling was much more rapid and severer. Gypsum crystals were clearly observable after 1 h, and the membrane surface was almost fully covered by scalants after 2 h. It is also interesting to note the difference in crystal sizes for two SI values. At SI = 1.97, the crystals were small (~10 μm), and they did not grow significantly in size over time even though more crystals appeared. However, at SI = 2.44, elongated crystals were typically observed (typically length ~50 μm). The direct microscopic observation method was also able to provide the growth of the crystal size over time (Fig. B in the appendix).

3.2. Effect of gypsum SI and ionic strength

In order to further study the effect of SI on FO scaling, we conducted gypsum scaling tests with different FS SI (ranging from 0.21 to 2.44 by adjusting the Ca^{2+} and SO_4^{2-} concentrations). Fig. 3(a) presents the behavior of FO water flux in AL-FS over time for

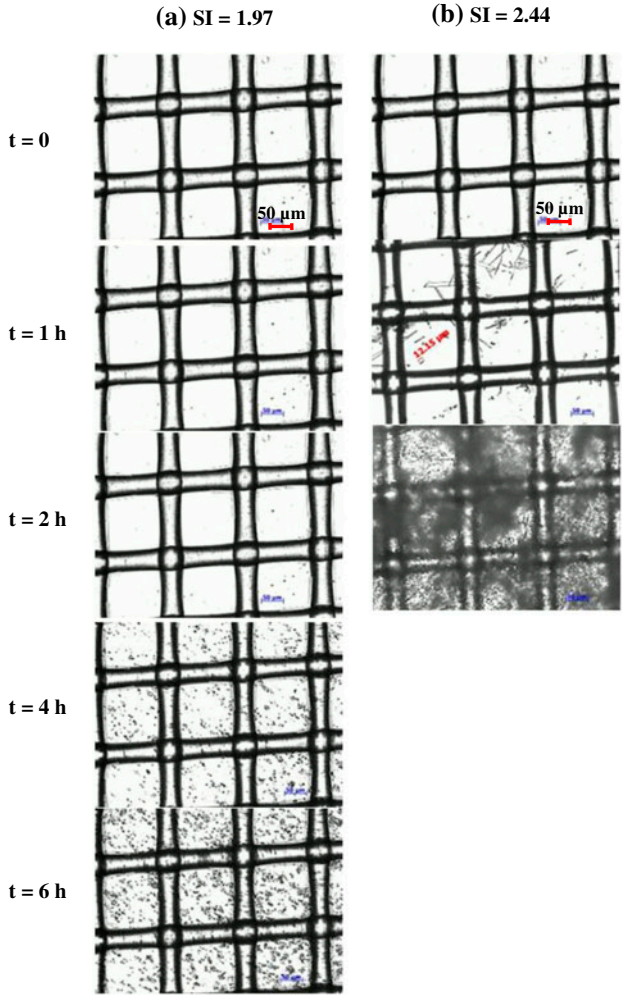

Fig. 2. Micrographs of gypsum crystal development with time under different feed solution SI: (a) SI = 1.97; (b) SI = 2.44. Experimental conditions: initial flux (~13 ± 1 L/m^2 h); cross-flow velocity of 9.75 cm/s; temperature at 23 ± 1 °C; FS pH at 7.5; ionic strength at 0.55 M; membrane orientation AL-FS.

different gypsum SI levels, and Fig. 3(b) shows the corresponding surface coverage by scalants obtained from image analysis of the optical micrographs. For SI = 0.21, a small flux decline of ~10% occurred over the 6 h fouling duration. No scaling was observed during the entire test run, which was expected since gypsum was under saturated. The small flux decline can be attributed to slight changes in DS and FS concentrations (i.e. the dilution of DS and concentration of FS) over time [6,26]. Consequently, the flux curve at SI = 0.21 was used as the baseline (no scaling condition) in the current study, and the difference between a scaling flux curve and the baseline can be attributed to scalant development.

In general, FO scaling was greatly affected by the feed SI, and scaling became more severe at increased SI (Fig. 3(a) and (b)). Compared to the baseline, flux reduction at SI of 1.53, 1.76, and 1.97 was relatively mild (Fig. 3(a)). Little flux reduction was observed in the first 3 h, while flux decline became more noticeable after this initial induction time. At SI ≥ 2.04, severe flux loss (≥50%) occurred and the scaling induction time was also shorter. The surface coverage plot (Fig. 3(b)) correlated very well with the flux decline curves. For SI ranging 1.53–1.97, surface coverage by scalants was negligible in the first 2–3 h, and small amount of scalants (up to 15% surface coverage) start to be noticeable at time >3 h. Surface coverage was much higher and occurred earlier for SI ≥ 2.04, which was in very good agreement with FO flux behavior. The severe flux decline at high SI feed water condition was attributed to the formation of an extensive cake layer of gypsum crystals. The strong dependence of FO scaling on SI is also consistent with the RO and PRO scaling literature [30,42,43].

In addition to the change of Ca^{2+} and SO_4^{2-} concentrations, the gypsum SI can also be affected by the solution ionic strength. Fig. 4 compares the FO scaling behavior for two different solution ionic strength values (0.55 and 0.15 M) by adjusting the NaCl concentration. The Ca^{2+} and SO_4^{2-} concentrations were fixed at 0.04 and 0.1 M, respectively. The flux curves for the two FS were compared in Fig. 4(a). A severe flux decline was observed at ~5 h for the low ionic strength (0.15 M) FS. This flux behavior is consistent with the sharp increase in surface coverage at 5 h under low IS condition (Fig. 4(b)). The microscopic images captured at the end of the experiments are compared in Fig. 5. More crystals and bigger crystal size were found on the membrane surface for 0.15 M FS (Fig. 5(a)). The current study suggests that, for fixed concentrations of scaling precursors, lowering ionic strength induces more severe scaling. Similar effect of ionic strength on scaling was reported previously for the scaling of nanofiltration process [43]. This phenomenon can be attributed to the effect of ionic strength on SI. Since lowering ionic strength increases the activities of both Ca^{2+} and SO_4^{2-}, it results in an increased SI and thus more severe scaling at long scaling duration (6 h). Nevertheless, we observed more scalant surface coverage and more water flux decline for 0.55 M FS between 4 and 5 h. Increasing ionic strength seemed to shorten the induction time of scaling significantly, causing a more severe scaling during this transient stage. The shorter induction time observed at higher ionic strength of solution is consistent with Boerlage et al. [44] who attributed this effect to the reduced interfacial tension

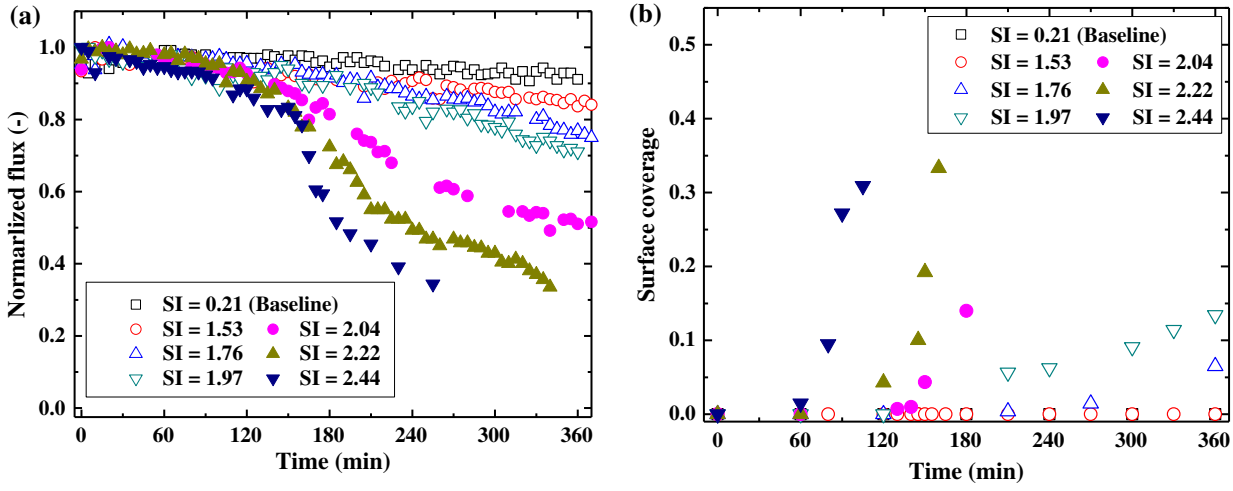

Fig. 3. Effect of FS SI on flux decline (a) and surface coverage by gypsum crystals (b). Experimental conditions: initial flux (~13 ± 1 L/m^2 h); cross-flow velocity of 9.75 cm/s; temperature at 23 ± 1°C; FS pH at 7.5; ionic strength at 0.55 M, membrane orientation AL-FS.

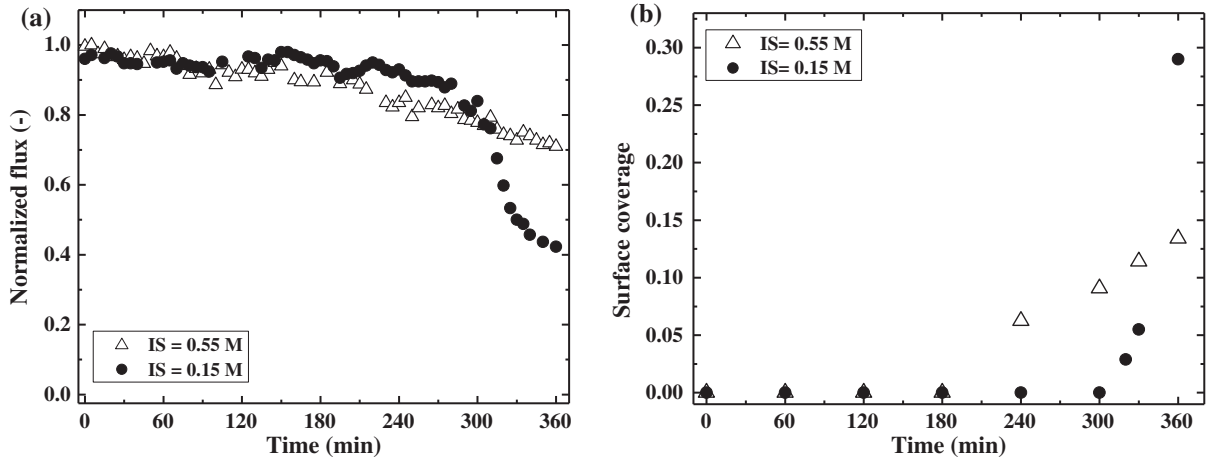

Fig. 4. Effect of ionic strength of the FS on flux decline (a) and surface coverage by gypsum crystals (b). Experimental conditions: initial flux (~13 ± 1 L/m^2 h); cross-flow velocity of 9.75 cm/s; temperature at 23 ± 1°C; FS pH at 7.5; 0.04 M Ca^{2+} and 0.1 M SO_4^{2-} in FS, membrane orientation AL-FS.

at higher ionic strength, which promotes nucleation of crystals. The current study may imply different scaling behaviors for seawater and brackish water desalination, with likely longer induction time but more severe long-term scaling for the latter.

3.3. Effect of membrane orientation

The effect of membrane orientation is discussed under the current section. For an FS SI of 1.97, the flux for the AL-FS orientation was relatively stable. In contrast, a nearly 50% flux reduction occurred in the first hour for the AL-DS orientation (Fig. 6(a)). Interestingly, the scalant surface coverage (Fig. 6(b) and Fig. C in the appendix) shows an opposite trend—the coverage was much lower for the AL-DS orientation despite the much more severe flux decline in this orientation. This suggests that different scaling mechanisms may exist for two orientations. Scaling in AL-FS orientation generally happens on the dense rejection layer and is dominated by the formation of a cake layer of crystals. The relatively stable flux behavior observed in this orientation is attributed to the smooth surface of the membrane rejection layer and its low tendency to interact with the scalants [27]. In addition,

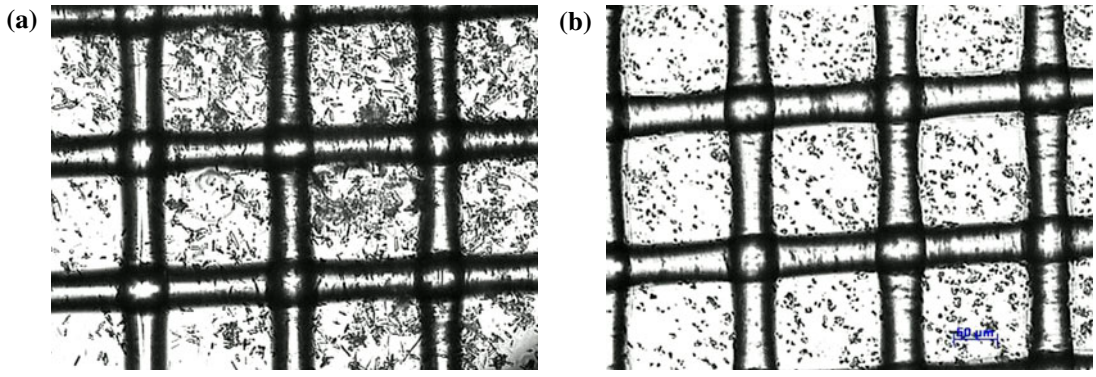

Fig. 5. Micrographs of scaled FO membranes at two ionic strength levels (0.15 M (a) and 0.55 M (b)). Experimental conditions: initial flux (~13 ± 1 L/m^2 h); cross-flow velocity of 9.75 cm/s; temperature at 23 ± 1 °C; FS pH at 7.5; 0.04 M Ca^{2+} and 0.1 M SO_4^{2-} in FS, membrane orientation AL-FS.

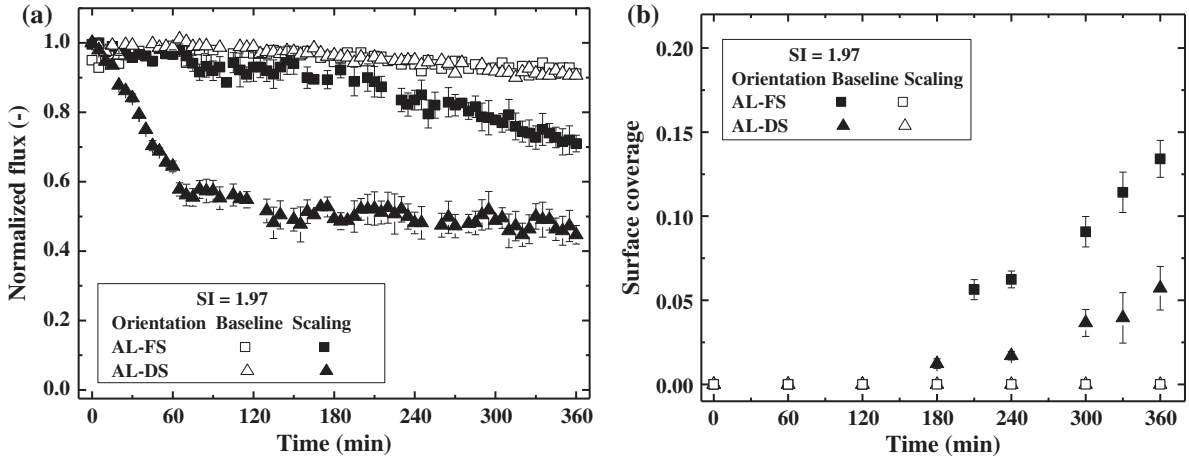

Fig. 6. Effect of membrane orientation on flux decline (a) and surface coverage by gypsum crystals (b). Experimental conditions: initial flux (~13 ± 1 L/m^2 h); cross-flow velocity of 9.75 cm/s; temperature at 23 ± 1 °C; FS pH at 7.5; ionic strength at 0.55 M; FS SI at 1.97.

the ICP self-compensation effect also helps to stabilize the FO flux in AL-FS [26]. A slight reduction in flux can result in a significantly reduced ICP (i.e. increased effective osmotic driving force) in AL-FS, resulting in a more inherently stable flux for this orientation.

The more severe FO scaling in AL-DS is consistent with previous studies on FO organic fouling [6,26] and PRO scaling [30]. In this orientation, the porous support structure is exposed to the FS. Scaling precursors (Ca^{2+} and SO_4^{2-} in the current study) can easily enter into the porous support structure before they are retained by the dense rejection layer. This causes a severe ICP of the scaling precursors and thus elevates SI inside the porous support. As a result, the AL-DS orientation is prone to internal scaling in the support layer. The above hypothesis is confirmed by the SEM cross-sectional images of the scaled membranes (Fig. 7). For the membrane tested in the AL-FS orientation, we could not observe any crystals inside the support layer. In contrast, crystals were present in the support layer for the membrane tested in AL-DS. According to Tang and co-workers [26,45], the internal clogging in AL-DS not only increases the membrane hydraulic resistance but also enhances ICP due to its modification to the pore structures of the support layer, leading to a synergistic effect on flux reduction. This explains why AL-DS suffered more flux reduction (Fig. 6(a)) even though less crystal formation was observed for this orientation (Fig. 6(b)). The ICP induced internal scaling in the AL-DS orientation and also explains why the flux reduction slowed down with time—the severe flux reduction in the first hour

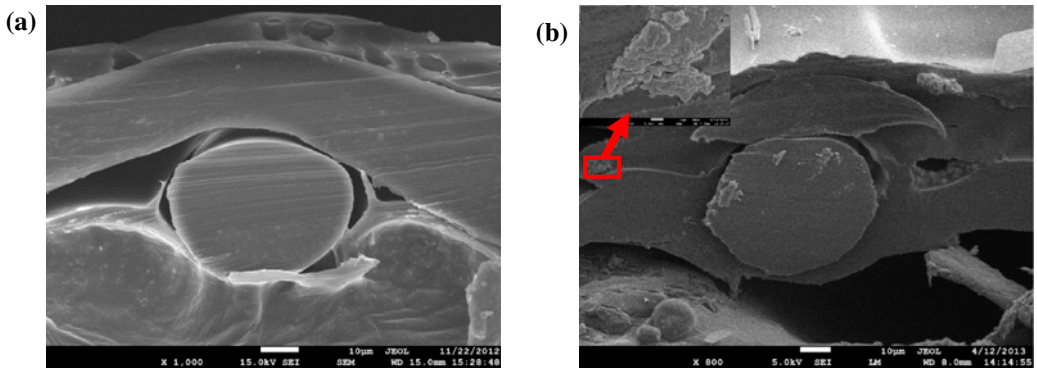

Fig. 7. SEM cross-sections of FO membranes scaled in AL-FS (a) and AL-DS (b) orientations. Experimental conditions: initial flux (~13 ± 1 L/m^2 h); cross-flow velocity of 9.75 cm/s; temperature at 23 ± 1 ℃; FS pH at 7.5; ionic strength at 0.55 M; FS SI at 1.97.

of scaling test resulted in greatly reduced ICP of scaling precursors and thus more stable flux behavior at the later stage of the test (Fig. 6).

According to the current study, operating FO in AL-DS shall be avoided due to its much greater propensity for scaling in addition to organic fouling. The current study also has important implications for PRO processes. The existing literature generally suggests the use of AL-DS orientation for PRO. However, in viewing higher organic fouling [46] and scaling tendency [30] of AL-DS, the AL-FS orientation may be preferred when using FSs prone to fouling (e.g. high organic content or high scaling precursor concentrations).

3.4. Scaling control: AS addition and rinsing under cross-flow conditions

The addition of AS has been proven to be an effective method for retarding scaling in RO process [47–49]. In this study, a 2 ppm AS was dosed in the FS in order to see its effectiveness on FO scaling control. The flux behavior with and without AS addition is presented in Fig. 8(a), and the corresponding scalant surface coverage is shown in Fig. 8(b). At an FS SI of 2.44, the AS dosage showed obvious scaling retarding effect. Without AS dosing, more than 60% flux reduction occurred (Fig. 8(a)) and the induction time was as short as 1 h (Fig. 8(b)). Gypsum crystals covered the

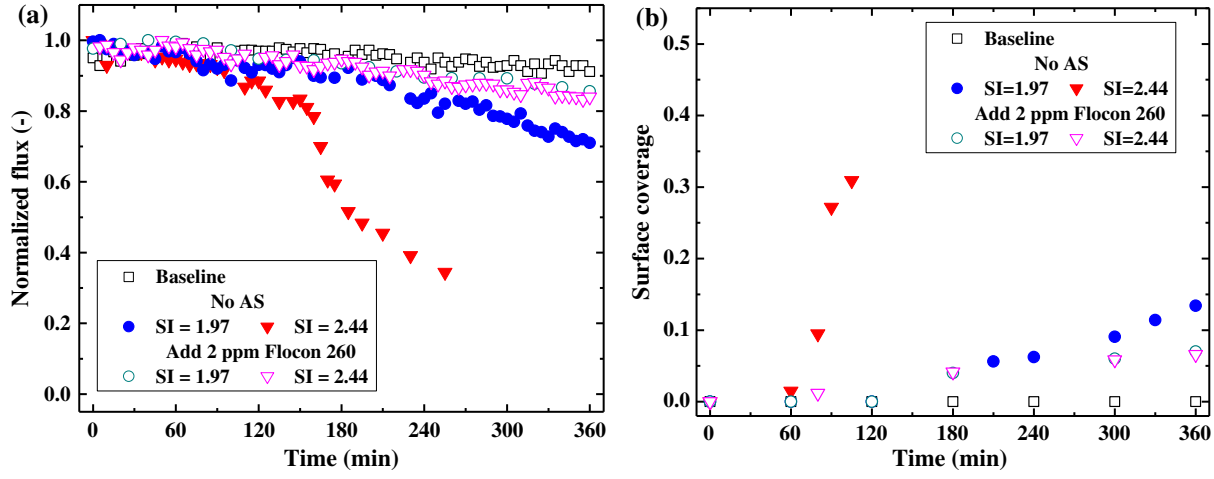

Fig. 8. Effect of AS addition on flux decline (a) and surface coverage by gypsum crystals (b). Experimental conditions: initial flux (~13 ± 1 L/m^2 h); cross-flow velocity of 9.75 cm/s; temperature at 23 ± 1 ℃; FS pH at 7.5; ionic strength at 0.55 M; membrane orientation AL-FS.

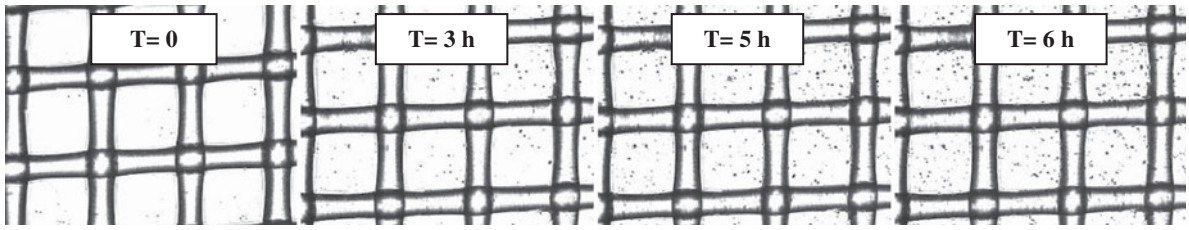

Fig. 9. Development of gypsum crystals for SI at 2.44 with addition of 2 ppm AS in FS. Experimental conditions: initial flux (~13 ± 1 L/m^{2}h); cross-flow velocity of 9.75 cm/s; temperature at 23 ± 1°C; FS pH at 7.5; ionic strength at 0.55 M; membrane orientation AL-FS.

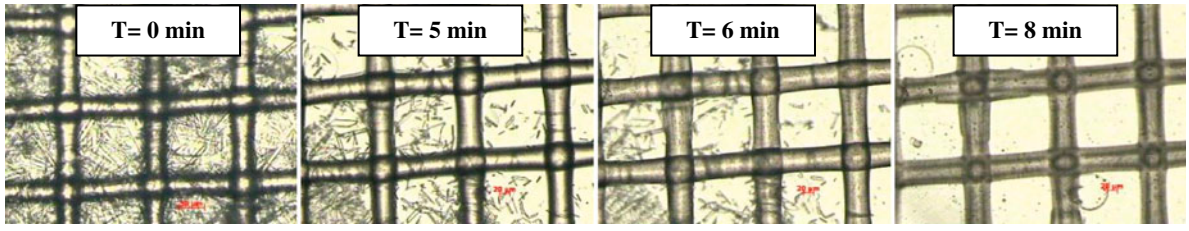

Fig. 10. Removing of gypsum crystals by water flush at end of experiment. Experimental conditions: initial flux (~13 ± 1 L/m^{2}h); cross-flow velocity of 9.75 cm/s; temperature at 23 ± 1°C; FS pH at 7.5; ionic strength at 0.55 M; membrane orientation AL-FS, FS SI at 2.44.

membrane surface rapidly after this initial induction time (Fig. 2). The addition of AS prolonged the induction time to be >2 h. The increase in surface coverage was more gradual with addition of AS (Fig. 9), which agrees well with the relatively moderate flux decline profile. Similar trend was also observed at a lower FS SI of 1.97, although effectiveness of AS was less obvious presumably due to the lower scaling tendency of the feed water. The current study confirms the effectiveness of AS addition for FO scaling control. Future studies are warranted to optimize AS types and dosages for prolonged FO operation.

In addition to AS dosage, we also tested the effectiveness of cleaning the scaled membrane by rinsing with deionized water under cross-flow conditions. Images shown in Fig. 10 depict the disappearance of the gypsum crystals that was formed under a severe scaling condition (SI = 2.44, no AS dosage, and AL-FS orientation). Despite that the membrane was heavily covered with gypsum crystals at time 0 (right before flushing), most of the crystals disappeared in merely 8 min, suggesting that simple flush under cross-flow conditions can be a very effective way for cleaning of FO scaling.

4. Conclusions

This study investigated the effect of FS SI and ionic strength, membrane orientation, and AS addition on gypsum scaling in FO process. In addition to FO water flux measurements, a direct microscopic observation system was used to characterize the scaling development. The microscopic observation was proven to be a useful tool for both qualitative and quantitative (via surface coverage analysis) monitoring of FO scaling. The results in the current study show that:

(1) Higher FS SI induced more severe scaling with rapid flux decline, shorter induction time, and increased number and size of gypsum crystals on the FO membrane surface.
(2) At fixed concentrations of calcium and sulfate, reducing the ionic strength of the FS prolonged the induction time of gypsum scaling. Nevertheless, scaling at longer duration (6 h) was more severe, which can be attributed to the increased FS SI as a result of higher ion activities.
(3) The AL-DS orientation suffered from internal scaling as a result of ICP of scaling precursors in the membrane support layer. The ICP induced scaling can promote severe FO flux reduction.
(4) Compared to the AL-DS orientation, the AL-FS orientation had more stable flux. Consistent with FO organic fouling results, the current study suggests that AL-FS is the preferred orientation for FO operation.
(5) The addition of AS was found to be effective in retarding FO scaling.

Acknowledgments

The authors thank the Singapore Ministry of Education (grant No. MOE2011-T2-2-035, ARC 3/12) for the financial support of the work. The authors also thank HTI for supplying membrane samples.

References

[1] T.Y. Cath, A.E. Childress, M. Elimelech, Forward osmosis: Principles, applications, and recent developments, J. Membr. Sci. 281 (2006) 70–87.
[2] S. Gormly, J. Herron, M. Flynn, M. Hammoudeh, H. Shaw, Forward osmosis for applications in sustainable energy development, Desalin. Water Treat. 27 (2011) 327–333.
[3] S. Zhao, L. Zou, C.Y. Tang, D. Mulcahy, Recent developments in forward osmosis: Opportunities and challenges, J. Membr. Sci. 396 (2012) 1–21.
[4] K.L. Lee, R.W. Baker, H.K. Lonsdale, Membranes for power generation by pressure-retarded osmosis, J. Membr. Sci. 8 (1981) 141–171.
[5] J. Wei, X. Liu, C.Q. Qiu, R. Wang, C.Y.Y. Tang, Influence of monomer concentrations on the performance of polyamide-based thin film composite forward osmosis membranes, J. Membr. Sci. 381 (2011) 110–117.
[6] B. Mi, M. Elimelech, Chemical and physical aspects of organic fouling of forward osmosis membranes, J. Membr. Sci. 320 (2008) 292–302.
[7] B.X. Mi, M. Elimelech, Organic fouling of forward osmosis membranes: Fouling reversibility and cleaning without chemical reagents, J. Membr. Sci. 348 (2010) 337–345.
[8] E.R. Cornelissen, D. Harmsen, K.F. De Korte, C.J. Ruiken, J.J. Qin, H. Oo, L.P. Wessels, Membrane fouling and process performance of forward osmosis membranes on activated sludge, J. Membr. Sci. 319 (2008) 158–168.
[9] A. Achilli, T.Y. Cath, E.A. Marchand, A.E. Childress, The forward osmosis membrane bioreactor: A low fouling alternative to MBR processes, Desalination 239 (2009) 10–21.
[10] W.C.L. Lay, Q.Y. Zhang, J.S. Zhang, D. Mcdougald, C.Y. Tang, R. Wang, Y. Liu, A.G. Fane, Study of integration of forward osmosis and biological process: Membrane performance under elevated salt environment, Desalination 283 (2011) 123–130.
[11] J.R. Mccutcheon, R.L. Mcginnis, M. Elimelech, Desalination by ammonia–carbon dioxide forward osmosis: Influence of draw and feed solution concentrations on process performance, J. Membr. Sci. 278 (2006) 114–123.
[12] C.H. Tan, H.Y. Ng, A novel hybrid forward osmosis—nanofiltration (FO–NF) process for seawater desalination: Draw solution selection and system configuration, Desalin. Water Treat. 13 (2010) 356–361.
[13] V. Yangali-Quintanilla, Z.Y. Li, R. Valladares, Q.Y. Li, G. Amy, Indirect desalination of Red Sea water with forward osmosis and low pressure reverse osmosis for water reuse, Desalination 280 (2011) 160–166.
[14] A. Achilli, T.Y. Cath, A.E. Childress, Power generation with pressure retarded osmosis: An experimental and theoretical investigation, J. Membr. Sci. 343 (2009) 42–52.
[15] Y. Xu, X.Y. Peng, C.Y.Y. Tang, Q.S.A. Fu, S.Z. Nie, Effect of draw solution concentration and operating conditions on forward osmosis and pressure retarded osmosis performance in a spiral wound module, J. Membr. Sci. 348 (2010) 298–309.
[16] Q.H. She, X. Jin, C.Y.Y. Tang, Osmotic power production from salinity gradient resource by pressure retarded osmosis: Effects of operating conditions and reverse solute diffusion, J. Membr. Sci. 401 (2012) 262–273.
[17] C.Y. Tang, Y.N. Kwon, J.O. Leckie, Fouling of reverse osmosis and nanofiltration membranes by humic acid—Effects of solution composition and hydrodynamic conditions, J. Membr. Sci. 290 (2007) 86–94.
[18] Y.N. Wang, C.Y. Tang, Fouling of nanofiltration, reverse osmosis, and ultrafiltration membranes by protein mixtures: The role of inter-foulant-species interaction, Environ. Sci. Technol. 45 (2011) 6373–6379.
[19] Z. Amjad, Applications of antiscalants to control calcium sulfate scaling in reverse osmosis systems, Desalination 54 (1985) 263–276.
[20] A. Al-Rammah, The application of acid free antiscalant to mitigate scaling in reverse osmosis membranes, Desalination 132 (2000) 83–87.
[21] M. Uchymiak, E. Lyster, J. Glater, Y. Cohen, Kinetics of gypsum crystal growth on a reverse osmosis membrane, J. Membr. Sci. 314 (2008) 163–172.
[22] S. Lee, J. Kim, C.H. Lee, Analysis of $CaSO_4$ scale formation mechanism in various nanofiltration modules, J. Membr. Sci. 163 (1999) 63–74.
[23] R.L. Mcginnis, M. Elimelech, Energy requirements of ammonia–carbon dioxide forward osmosis desalination, Desalination 207 (2007) 370–382.
[24] O.A. Bamaga, A. Yokochi, B. Zabara, A.S. Babaqi, Hybrid FO/RO desalination system: Preliminary assessment of osmotic energy recovery and designs of new FO membrane module configurations, Desalination 268 (2011) 163–169.
[25] S. Zou, Y.S. Gu, D.Z. Xiao, C.Y.Y. Tang, The role of physical and chemical parameters on forward osmosis membrane fouling during algae separation, J. Membr. Sci. 366 (2011) 356–362.
[26] C.Y.Y. Tang, Q.H. She, W.C.L. Lay, R. Wang, A.G. Fane, Coupled effects of internal concentration polarization and fouling on flux behavior of forward osmosis membranes during humic acid filtration, J. Membr. Sci. 354 (2010) 123–133.
[27] B.X. Mi, M. Elimelech, Gypsum scaling and cleaning in forward osmosis: Measurements and mechanisms, Environ. Sci. Technol. 44 (2010) 2022–2028.
[28] S.F. Zhao, L.D. Zou, Effects of working temperature on separation performance, membrane scaling and cleaning in forward osmosis desalination, Desalination 278 (2011) 157–164.
[29] E. Arkhangelsky, F. Wicaksana, S.R. Chou, A.A. Al-Rabiah, S.M. Al-Zahrani, R. Wang, Effects of scaling and cleaning on the performance of forward osmosis hollow fiber membranes, J. Membr. Sci. 415 (2012) 101–108.
[30] M. Zhang, D. Hou, Q. She, C.Y. Tang, Gypsum scaling in pressure retarded osmosis: Experiments, mechanisms and implications, Water Res. 48 (2014) 387–395.

[31] Y.L. Liu, B.X. Mi, Combined fouling of forward osmosis membranes: Synergistic foulant interaction and direct observation of fouling layer formation, J. Membr. Sci. 407 (2012) 136–144.
[32] E. Arkhangelsky, F. Wicaksana, C. Tang, A.A. Al-Rabiah, S.M. Al-Zahrani, R. Wang, Combined organic-inorganic fouling of forward osmosis hollow fiber membranes, Water Res. 46 (2012) 6329–6338.
[33] Y.P. Zhang, A.W.K. Law, A.G. Fane, Determination of critical flux by mass balance technique combined with direct observation image analysis, J. Membr. Sci. 365 (2010) 106–113.
[34] Y.N. Wang, F. Wicaksana, C.Y. Tang, A.G. Fane, Direct microscopic observation of forward osmosis membrane fouling, Environ. Sci. Technol. 44 (2010) 7102–7109.
[35] ASTM, D1141—98: Standard Practice for the Preparation of Substitute Ocean Water, ASTM International, 2008.
[36] A. Rahardianto, B.C. Mccool, Y. Cohen, Reverse osmosis desalting of inland brackish water of high gypsum scaling propensity: Kinetics and mitigation of membrane mineral scaling, Environ. Sci. Technol. 42 (2008) 4292–4297.
[37] Oli, OLI Stream Analyzer Software Version 2, OLI Systems Inc., Morris Plains, NJ, 2005.
[38] S. Ben Ahmed, M.M. Tlili, N. Ben Amor, Influence of a polyacrylate antiscalant on gypsum nucleation and growth, Cryst. Res. Technol. 43 (2008) 935–942.
[39] S. Ghani, N.S. Al-Deffeeri, Impacts of different antiscalant dosing rates and their thermal performance in Multi Stage Flash (MSF) distiller in Kuwait, Desalination 250 (2010) 463–472.
[40] J. Wei, C. Qiu, C.Y. Tang, R. Wang, A.G. Fane, Synthesis and characterization of flat-sheet thin film composite forward osmosis membranes, J. Membr. Sci. 372 (2011) 292–302.
[41] Y.N. Wang, J. Wei, Q.H. She, F. Pacheco, C.Y.Y. Tang, Microscopic Characterization of FO/PRO Membranes —A comparative study of CLSM, TEM and SEM, Environ. Sci. Technol. 46 (2012) 9995–10003.
[42] S. Shirazi, C.-J. Lin, D. Chen, Inorganic fouling of pressure-driven membrane processes—A critical review, Desalination 250 (2010) 236–248.
[43] A.S. Al-Amoudi, Factors affecting natural organic matter (NOM) and scaling fouling in NF membranes: A review, Desalination 259 (2010) 1–10.
[44] S.F.E. Boerlage, M.D. Kennedy, I. Bremere, G.J. Witkamp, J.P. Van der Hoek, J.C. Schippers, Stable barium sulphate supersaturation in reverse osmosis, J. Membr. Sci. 179 (2000) 53–68.
[45] Q. She, X. Jin, Q. Li, C.Y. Tang, Relating reverse and forward solute diffusion to membrane fouling in osmotically driven membrane processes, Water Res. 46 (2012) 2478–2486.
[46] Q. She, Y.K.W. Wong, S. Zhao, C.Y. Tang, Organic fouling in pressure retarded osmosis: Experiments, mechanisms and implications, J. Membr. Sci., 428 (2013) 181–189.
[47] W.-Y. Shih, K. Albrecht, J. Glater, Y. Cohen, A dual-probe approach for evaluation of gypsum crystallization in response to antiscalant treatment, Desalination 169 (2004) 213–221.
[48] E. Lyster, M.-M. Kim, J. Au, Y. Cohen, A method for evaluating antiscalant retardation of crystal nucleation and growth on RO membranes, J. Membr. Sci. 364 (2010) 122–131.
[49] A. Antony, J.H. Low, S. Gray, A.E. Childress, P. Le-Clech, G. Leslie, Scale formation and control in high pressure membrane water treatment systems: A review, J. Membr. Sci. 383 (2011) 1–16.

Appendix

Fig. A presents the XRD analysis of the scalant found in the current study based on the XRD pattern, it is confirmed that the scalant was gypsum.

Fig. B shows the growth of gypsum crystals over time for a FS SI of 2.44. In the first 40 min of the scaling test, gypsum crystals were hardly observed on the membrane surface. Small crystals (~10 μm in length) were observed at ~1 h, and these crystals grew in size with time in a nearly linear fashion.

Fig. C presents the optical micrographs of scaled membranes in both AL-DS and AL-FS orientation. Less surface coverage was observed for the AL-DS orientation. However, this orientation was more prone to internal scaling (Fig. 7), which caused severe flux reduction compared to the AL-FS orientation.

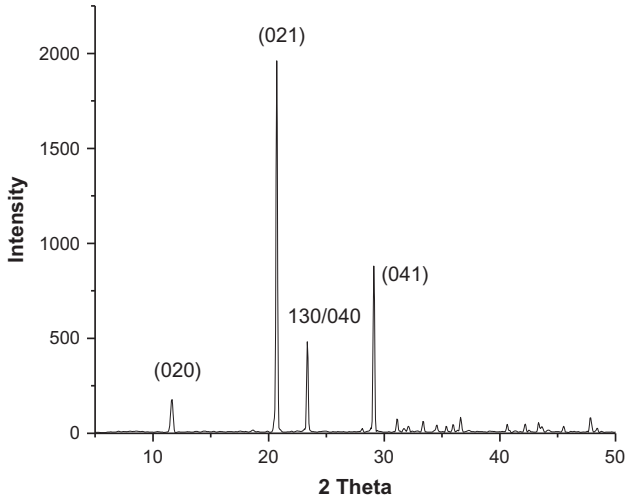

Fig. A. XRD spectrum of scalants. The observed XRD pattern was consistent with that of gypsum, confirming that gypsum was the only crystalline phase in the current study.

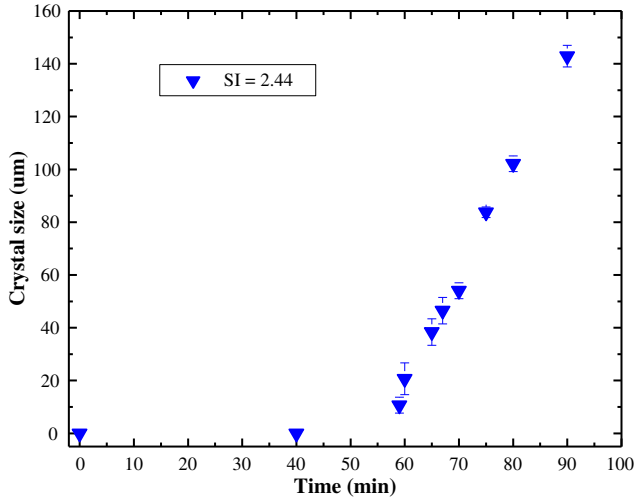

Fig. B. A single gypsum crystal development with time under FS SI = 2.44. Experimental conditions: initial flux (~13 ± 1 L/m^2 h); cross-flow velocity of 9.75 cm/s; temperature at 23 ± 1 ℃; FS pH at 7.5; ionic strength at 0.55 M.

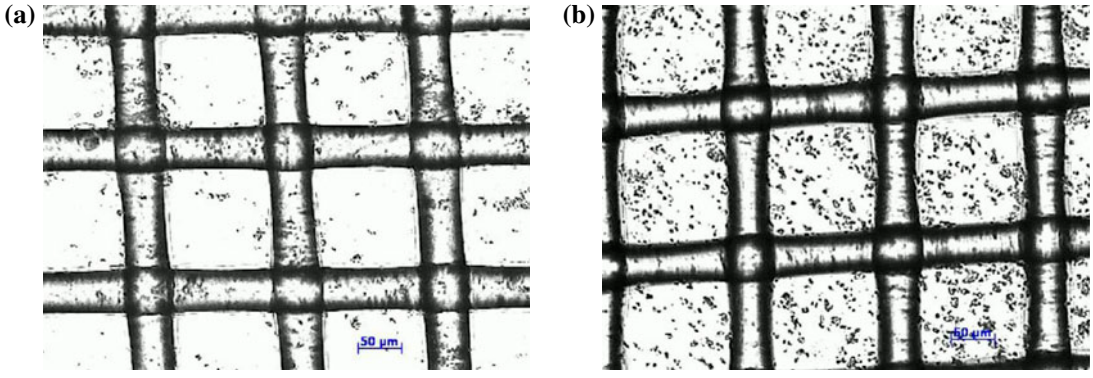

Fig. C. Effect of membrane orientation surface coverage by gypsum crystals. (a) AL-DS and (b) AL-FS orientations. Micrographs were taken after 6 h scaling experiment. Experimental conditions: initial flux (~13 ± 1 L/m^2 h); cross-flow velocity of 9.75 cm/s; temperature at 23 ± 1 ℃; FS pH at 7.5; ionic strength at 0.55 M; FS SI at 1.97.